Journal of Fluids and Structures (1998) **12,** 949–958
Article No. fl980177

UNSTEADY LIFT FORCE ON A TOWED SPHERE

G. C. LAUCHLE

Penn State University, Graduate Program in Acoustics and Applied Research Laboratory
P.O. Box 30, State College, PA 16804, U.S.A.

AND

A. R. JONES

General Electric Co., Appliance Park, AP3-220, Louisville, KY 40225, U.S.A.

(Received 30 January 1998 and in revised form 24 August 1998)

An experimental effort to characterize the broadband flow-induced lift forces on a spherical body that is towed underwater is described. The body itself is the transducer which is comprised of a small geophone encased in a near-neutrally-buoyant sphere, 7·62 cm in diameter. The research described in this paper quantifies the flow-induced unsteady lift force signal as a function of the sphere diameter Reynolds number ($7620 < \mathrm{Re} < 34\,290$) and the Strouhal number ($1{\cdot}5 < \mathrm{St} < 30$). It is found that the broadband flow-induced unsteady lift forces are proportional to the product of an area and the dynamic pressure of the flow, as expected. These data are compared to similar data measured previously on a finite-length, right-circular cylinder in cross flow. This comparison indicates that the cylindrical body creates more unsteady side force than does the spherical one, particularly at the lower end of the Strouhal number range. © 1998 Academic Press

1. INTRODUCTION

VARIOUS NOISE SOURCES are known to affect the performance of drifting or moored hydrophones. In quiescent fluid, these sources include ambient background noise, electronic noise, and transducer suspension-induced noise. Because of ocean currents induced by tides, gravity, temperature gradients, or surface waves, many real-world situations result in a fluid that is not quiescent. Typical currents in the ocean have mean velocities ranging from 0·25 to 0·5 knots. It has been shown by Finger *et al.* (1979), McEachern (1980), and McEachern & Lauchle (1995) that this fluid flow can cause an additional flow-induced self-noise in the sensor that can dominate all the other sources combined. Flow-induced noise on hydrophones configured as bluff bodies depends strongly on the flow velocity, Reynolds number, sensor geometry, and Strouhal number. (Recall that the Reynolds number, $\mathrm{Re} = UD/\nu$, where U is the mean flow velocity, D is body diameter, and ν is the kinematic viscosity of the fluid; the Strouhal number, $\mathrm{St} = fD/U$, where f is the frequency in Hz.) In the absence of flow and other extraneous noise sources, the output from the hydrophone is the acoustic signal generated by a propagating wave of interest. However, when flow is present, hydrodynamic disturbances from large- and small-scale instabilities, vortex shedding, and turbulent velocity fluctuations can occur simultaneously on the surface of the hydrophone and in the near wake. These disturbances impart unsteady forces on the sensor itself, creating a flow-induced self-noise signal which contaminates or "masks" the desired acoustic signal.

Acoustic signals of interest in the ocean usually originate from a distance source; therefore, hydrophone directional sensitivity is oftentimes an important consideration in

0889–9746/98/080949 + 10 $30.00/0 © 1998 Academic Press

undersea acoustic measurements. Pressure gradient and/or acoustic velocity hydrophones have a desirable directional axis of peak response (even at infrasonic and low frequencies). They can also be used in conjunction with a pressure sensor to infer intensity and propagation direction (Gabrielson *et al.* 1995a, b). Berliner & Lindberg (1995) have compiled a collection of papers reporting that acoustic velocity sensors are often used in lieu of omni-directional pressure hydrophones in many undersea applications. However, Finger *et al.* (1979), McEachern (1980), and Keller (1977) show that acoustic particle velocity (or pressure gradient) hydrophones exhibit a considerably higher sensitivity to flow effects than do pressure hydrophones. Keller (1977) quoted differences of approximately 50 dB at 10 Hz for a flow speed of 0·5 knots. These authors, in addition to Gabrielson *et al.* (1995b) and McEachern & Lauchle (1995), have shown that the flow-induced self-noise signal from an acoustic velocity sensor is directly related to the hydrodynamically induced body forces generated by the flow over the hydrophone. This, of course, is not unexpected because the sensors are inertial sensors. The measured unsteady velocity is related to the body acceleration by a frequency factor, and this relates to the unsteady force from Newton's second law of motion.

Most of the previously published work has considered the cylindrical-shaped hydrophone in cross flow, although Finger *et al.* (1979) indicated that there was little difference between the flow noise spectrum of a cylindrical pressure gradient hydrophone in cross flow and a spherical one. McEachern & Lauchle (1995) found that the cylinder aspect (length-to-diameter) ratio plays a key role in the flow-noise signal, as does the corner radius of the cylinder endcaps. The flow-induced fluctuating force levels decrease (to a degree) as these parameters are increased.

Based on this finding, and the apparent indifference noted by Finger *et al.* (1979) between a cylinder and a sphere, it is important to investigate more thoroughly the flow-induced forces generated by uniform flow over a sphere. Using typical water velocities of ocean currents ($0{\cdot}25\ \text{kt} < U < 0{\cdot}5\ \text{kt}$), and a range of sphere diameters considered in applications, the Reynolds number range of interest would be approximately $5000 < \text{Re} < 30\,000$ (here, $\nu = 10^{-6}\ \text{m}^2/\text{s}$). The frequency range would be similar to that of the previous investigations ($10\ \text{Hz} < f < 100\ \text{Hz}$), which results in a Strouhal number range of 1·5–30. This range is considerably higher than the characteristic vortex shedding frequency range of a sphere. The unsteady force spectra are broadband in this range of Strouhal numbers.

The objective of the research presented in this paper is to characterize experimentally (and within the Reynolds and Strouhal number ranges noted above) the flow-induced unsteady side (lift) forces created on a spherical body configured as an acoustic particle velocity hydrophone operating underwater. The acquired spectral data are nondimensionalized and compared to similar nondimensional force spectral data obtained by McEachern & Lauchle (1995) for finite-length cylinders in cross flow. The fluid mechanics of a sphere depends in a rather complex way on the Reynolds number range also, so we will summarize those effects first.

2. FLUID FLOW REGIMES OF A SPHERE

The wake structure behind a sphere is more complex than that of a long cylinder. Extensive research has been conducted and vast amounts of experimental data have been accumulated. Of note, was the identification (Möller 1938; Taneda 1956; Achenbach 1974) of more than one characteristic vortex shedding frequency from a sphere. This has led to the definition of both high- and low-mode Strouhal numbers. Kim & Durbin (1988) identified these two modes as coexisting and due to the following.

(i) a vortex shedding associated with the large-scale instability in the wake. The shedding frequency of this mode, when nondimensionalized in the form of a Strouhal number is practically independent of Reynolds number. For $400 \leq \mathrm{Re} \leq 10^5$, the Strouhal number for this mode is of order 0·2.

(ii) The second instability frequency is greater than the first, and is due to a small-scale instability associated with the separating shear layer. The Strouhal number for this mode increases logarithmically with Reynolds number, although it is indistinguishable from and equal to that of the lower mode for $\mathrm{Re} \leq 800$. This small-scale instability frequency is sometimes difficult to detect at higher Reynolds numbers too ($\mathrm{Re} \geq 15\,000$), because of masking by other broadband velocity fluctuations associated with the near wake.

The various flow regimes for a sphere, as summarized by Sakamoto & Haniu (1990) are as follows.

$Re < 5$. This is the region of Stokes flow which is completely driven by viscous forces. These forces are proportional to the product of the viscosity, velocity, and characteristic length (diameter).

$5 < Re < 300$. A wave-like laminar wake of very long period forms behind the sphere.

$300 < Re < 420$. A hairpin vortex begins to shed; a spectral peak shows up in the unsteady velocity spectrum.

$420 < Re < 480$. The shedding of the hairpin vortices becomes irregular. This is the early transition regime.

$480 < Re < 650$. The shedding mode is in a continuous state of randomness, or irregularity.

$650 < Re < 800$. The shedding pattern differs from that of lower Reynolds numbers due to a pulsation of the vortex sheet. Multiple frequencies are observed and the cores of the shed vortices begin to show signs of turbulence.

$800 < Re < 3000$. Some of the vortex tubes formed by the vortex sheet separating from the sphere surface enter into the vortex formation region, while others are shed in small vortex loops. The large-scale vortices move away from the sphere rotating at random about an axis parallel to the flow through the center of the sphere. The wake becomes turbulent at $\mathrm{Re} \sim 2000$.

$3000 < Re < 6000$. This is another transition region where the measured low-mode shedding Strouhal numbers decrease rapidly with increasing Reynolds number. The power spectrum of the fluctuating wake velocity shows one characteristic peak plus considerable broadband energy on both sides of this peak. The vortex sheet is changing from laminar to turbulent in this regime.

$6000 < Re < 370\,000$. The separated vortex sheet is now completely turbulent. The vortices shed from the formation region become stabilized because the separated shear layer is no longer laminar, but turbulent. This stabilization causes the velocity fluctuation spectrum to lose some of the broadband nature observed in the previous region. The Strouhal frequency of regular shedding increases with Reynolds number and then approaches the constant value of 0·19 at $\mathrm{Re} \sim 20\,000$.

In addition to these observations, Achenbach (1974) states that for Reynolds numbers between 6000 and 300 000 the vortex separation point rotates around the sphere. Taneda (1978) performed detailed flow visualization studies of the sphere wake in a Reynolds number range of 10^4–10^6 and found that the wake is not axisymmetric. He suggested, based on this and Achenbach's observations (rotating separation point), that a sphere subjected to uniform flow will have a completely random distribution of side forces.

For the frequencies, velocities, and length scales considered in the current study, the Reynolds number range falls within the range where random side (lift) forces are expected.

The Strouhal numbers are typically greater than 1·5, which are above the expected discrete vortex shedding ranges of the sphere. The data presented for the unsteady side forces are thus in a range of Strouhal numbers that has received very little attention in the past. The only other comparable data for this problem are presented by Willmarth & Enlow (1969). They determined unsteady sphere side forces and moments at Reynolds numbers greater than $4{\cdot}8 \times 10^5$, and for Strouhal numbers between approximately 10^{-4} and 0·2.

3. EXPERIMENTAL SETUP

3.1. The Spherical Test Model

In accordance to the design recommendations presented by Gabrielson *et al.* (1995b), a GeoSpace Corp., GS20-DH7 geophone (velocity sensor) was encased in a neutrally buoyant spherical body so as to create a sensor capable of sensing weak underwater acoustic velocity fluctuations. The spherical acoustic velocity transducer, shown in Figure 1, is cast from a 3·5 : 1 by volume mixture of polystyrene micro balloons and epoxy resin, which resulted in a slightly negatively buoyant body. The slightly negative buoyancy was desired so that ballast weights could be avoided during testing that may adversely affect the flow-induced force measurements.

The spherical sensor was calibrated for force in water by mechanically exciting it with a shaker. Comparison of the geophone output voltage with that of a standard accelerometer securely mounted to the spherical surface provided a transfer function that, when corrected for the known sensitivity of the accelerometer and the mass of the hydrophone, yields a sensitivity function of the hydrophone in the units of V/N. The measured force sensitivity of the test hydrophone is 0 dB re 1 V/N at 65 Hz. The sensitivity varies with frequency, as expected, at -6 dB/octave. When the sphere is towed underwater, the measured geophone voltage autospectrum is divided by this force sensitivity function to yield the desired unsteady side force autospectrum.

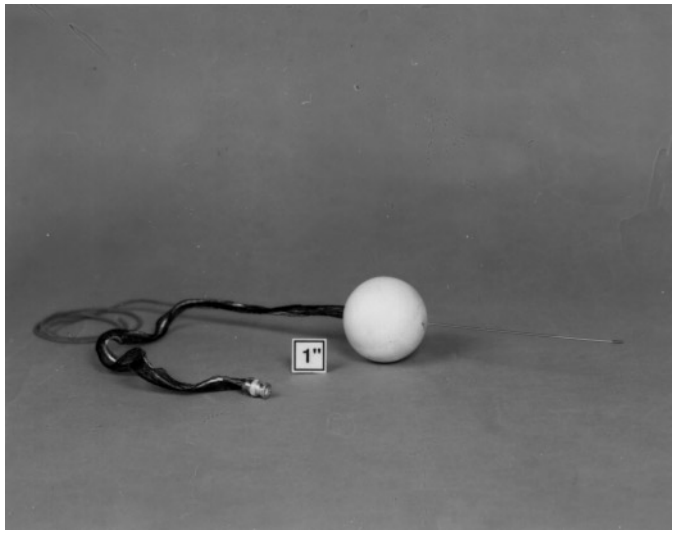

Figure 1. Photograph of the spherical velocity-sensitive sensor and test model. The long narrow rod on the bottom side was removed during testing. It was used only for the manufacturing process.

3.2. Tow Tank Facility

A long tow channel was developed specifically for the flow noise measurements performed in this study. Vibration isolation within the facility is critical because of the low-frequency range of interest, the low force levels being measured, and the extreme sensitivity of the acoustic velocity hydrophone to vibration. Therefore, much attention was given to the reduction of vibration from ambient noise sources and noise generated by the towing system itself. The tank, shown schematically in Figure 2 and photographically in Figure 3,

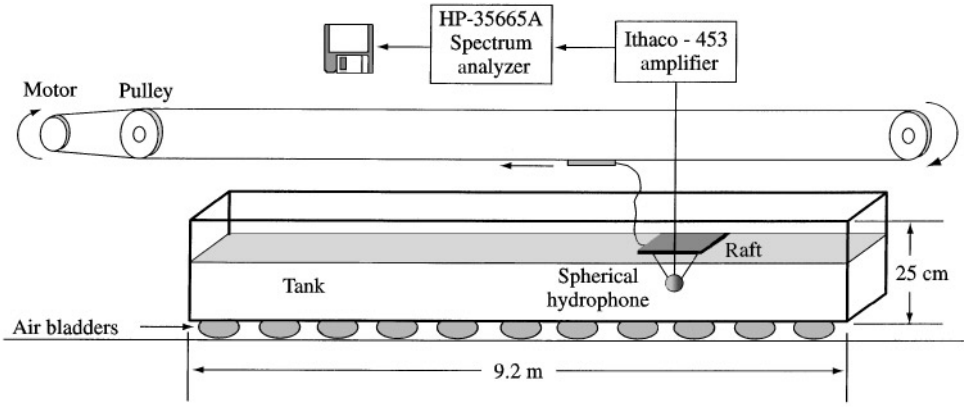

Figure 2. Schematic of the tow tank and data acquisition instrumentation.

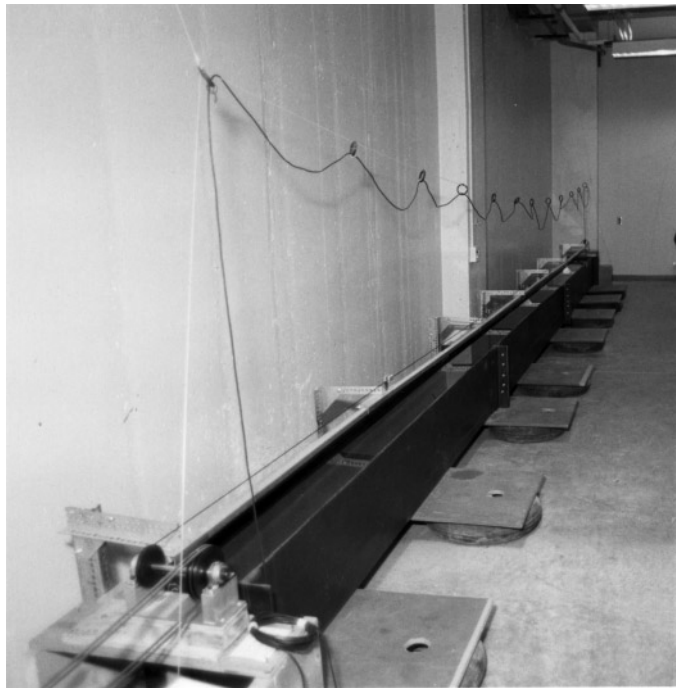

Figure 3. Photograph of the quiet tow tank facility showing its foundation of air-filled bladders and the monorail towing carriage.

sits on semi-inflated air bladders which rest on a concrete floor poured directly over bedrock in the basement of a laboratory building. This procedure effectively isolates the tank from seismic noise sources. A precision digitally controlled stepping motor drives a plastic coated cable the length of the tank. The cable is supported by a pulley mounted to the opposite wall. The motor has several stages of flexible shafts before being mechanically linked to the cable by two flexible driving belts. The only mechanical link from the tow cable to the tank is 3 mm diameter surgical rubber tubing, about 0·6 m in length, which extends from the cable to a smooth raft. A fin mounted on the back of the raft keeps it oriented properly. The sphere is suspended underneath the raft using 3X monofilament fishing line in a three-point suspension.

The geophone encased in the sphere is oriented normal to the flow direction so that side-to-side lift forces are sensed. Fluctuating drag forces are suppressed from the measurements because of the cosine directivity pattern of the geophone. We have elected not to measure the unsteady drag forces in this investigation because it is believed from this and other independent investigations that the side forces dominate the sensor self-noise signal. Support for this may be inferred from Taneda's (1978) observation of a random side-force field being produced by sphere wake nonaxisymmetry, and by Blake (1986) who states that the r.m.s. drag force of a cylinder is only 10% of the r.m.s. lift force. The side-to-side motion of the sphere at frequencies of 10 Hz or greater is extremely small, so blockage effects from the tank side walls were considered negligible. The width of the tank was four sphere diameters.

A small-diameter signal cable runs from the top of the sphere to the back of the raft. The signal cable is surrounded with nylon mesh to break up unwanted vortex shedding and instability frequencies associated with the cable itself. The signal cable continues from the raft to an overhead payout rig leading to an Ithaco (model 453) amplifier where the signal is amplified 50–70 dB before going to an HP-35665A FFT analyzer. A Hanning window was used in the analyzer which then provided power spectral density estimates in the 10–100 Hz frequency range with a 1 Hz resolution. Because of the limited time available for each towing run, no more than 20 spectral averages could be realized per run. Thus, to decrease the random error in the spectra, data from multiple towing runs were averaged together. The total number of ensembles was thus increased to 60 or more. The random error in spectrum level is inversely proportional to the square-root of the number of spectral averages, so the statistical variations due to randomness of the measured spectral levels is of order $\pm 0{\cdot}6$ dB. Because of the 1 Hz effective bandwidth of the spectral analysis, there is no bias error. The accuracy of the calibration values used to infer the unsteady forces is also of order ± 1 dB. Thus, the overall random error of the flow-induced forces presented is estimated to be of order ± 2 dB.

The flow over the spherical hydrophone is produced by towing it in a controlled manner in the long tow channel. The flow-induced sensor self-noise can be studied systematically with a constant diameter sensor by varying the tow velocity, and hence the Reynolds number. For tow speeds between 10 and 45 cm/s, the Reynolds number range is from 7620 to 34 290. The dependent variable is the fluctuating (lift) force imparted on the sphere by the unsteady velocity fluctuations caused by rectilinear motion in a quiescent and uniform body of liquid. The effects of inlet turbulence or the effects of non-fluid particles impacting the sphere are not considered.

3.3. System Background Noise

Experiments were conducted to assure that the measured unsteady forces induced by facility background noise (ambient plus mechanical noise) were below those measured on

the sphere when exposed to flow. To reduce the ambient noise floor, all flow noise measurements were made after normal working hours when the ventilation system of the building was not in operation and other extraneous noise sources were at a minimum. The mechanical system noise is defined as the output noise of the submerged, but mechanically disconnected and stationary, spherical sensor while the tow cable is operated at the normal towing speeds. The ambient noise is defined as the submerged, stationary sensor output at zero tow cable speed. Spectra for each of these contaminating noises were determined at velocities from 10 to 45 cm/s, in increments of 2·5 cm/s. They were compared then to the flow-induced lift spectra. For the majority of the test velocities and frequencies considered, the signal-to-ambient or mechanical noise ratio was well above 10 dB, indicating that the system noise is not contaminating the flow-noise data; see Jones (1996) for additional details. At some lower towing speeds, however, it was observed that the broadband fluctuating lift flow-noise levels approached the levels of the background noise. To assure that the flow-noise data presented are not background-noise-limited, portions of the measured flow-noise spectra are omitted if the background noise level is within 6 dB or less of the measured flow noise level.

4. RESULTS

Figure 4 shows a family of flow-induced lift spectra measured in fresh, clean water at different towing speeds. These conditions correspond to $7620 < \mathrm{Re} < 34\,290$. As noted in Section 3·3, portions of these individual spectra are necessarily omitted because of being within 6 dB of the background noise spectra corresponding to that particular towing speed. We note that a 6 dB or more signal-to-noise ratio is established for the entire frequency range at the higher Reynolds number conditions. The situation degrades—especially at the higher frequencies—as the tow speed is lowered below 20 cm/s.

4.1 Dimensionless Form of the Flow-Induced Lift Force Spectra

Because the Reynolds number is greater than 6000 turbulence is present in the near wake of the sphere. It would be expected then, that the force levels would scale on the inertial forces of the flow (the high Reynolds numbers required for turbulent flow imply that the inertial

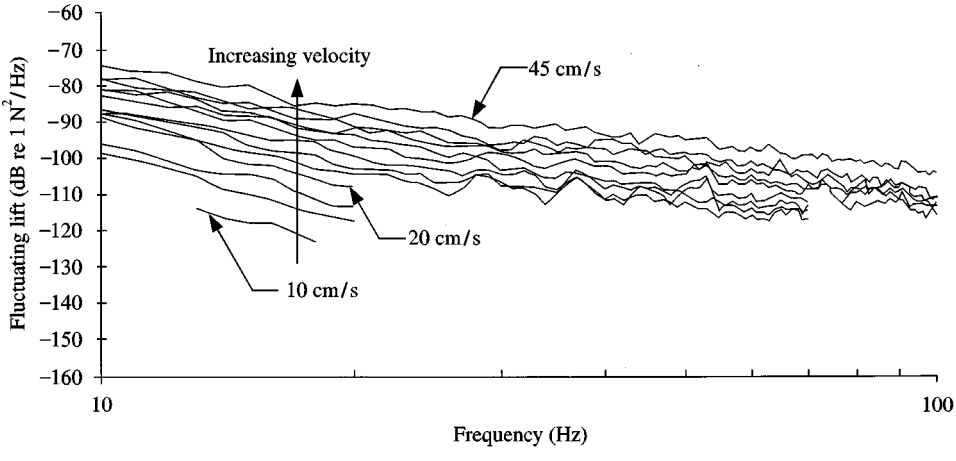

Figure 4. Autospectra of the fluctuating force sensed by the sphere in pure water for a range of flow velocities ($7620 < \mathrm{Re} < 34\,290$).

forces dominate the viscous forces). We adopt the same scaling as first proposed for hydrophone flow-induced self-noise by McEachern (1993). Denoting the one-sided auto-spectrum of the force fluctuations by $G_F(f)$, the dimensionless form of the power spectral density function would be $G_F(f)\ (U/D)/(\rho U^2 A)^2$ which is expressed as a function of the Strouhal number $\mathrm{St} = fD/U$. Here, ρ is the density of the liquid medium, A is the frontal area of the sphere exposed to flow, and St normalizes the frequency on the inertial time scale (D/U).

The spectra of Figure 4 are presented in the dimensionless inertial force spectrum format in Figure 5. The collapse of these spectra to the narrow band indicated suggests that the mechanism of flow-induced lift in this Reynolds and Strouhal number range is indeed the inertial forces created by the turbulent fluctuations in the separated vortex sheet. Such forces must also include those induced by the random rotation of the separation line and the resulting non-axisymmetry of the vortex structures downstream of separation. The Reynolds numbers shown here are below the boundary layer transition Reynolds number of a sphere ($\sim$300 000), so mechanisms due to transition or turbulent boundary layer pressure fluctuations are likely nonexistent.

Of particular interest are the flow-induced forces on a sphere compared to those of a cylinder in cross flow. Shown in Figure 5 are three straight lines representing the least mean-square fits of cylindrical sensor side force spectra (McEachern 1993) that were measured in a very quiet flooded quarry, and independently of the apparatus reported in this paper. The Reynolds number range for these experiments was 4000 to 18 000. The lower of the two spectra is for a cylinder having an aspect ratio of 1·0 and with rounded endcaps. The radius of the endcap corners is $R = 0{\cdot}25D$, where D was 10·16 cm. This was the "quietist" cylinder geometry identified by McEachern. The middle trace of the three cylinder flow noise spectra was measured for a geometric configuration that most closely matches a sphere; the aspect ratio was 1·5 and the endcaps were hemispheres ($R = D/2$). The dimensionless force spectrum for this basically elongated sphere is seen to fall slightly below the current data due to a steeper spectral slope. The higher of the three cylinder flow noise spectra is for a right-circular cylinder in cross flow, i.e., the aspect ratio is 1·0, but there is no corner radius ($R = 0$). At the lower values of St, this cylindrical sensor generates more flow noise than the spherical sensor.

As one additional comparison of the subject experimental findings to an independently acquired data set, we refer to Figure 6. The dimensionless (lift) force spectra of the current

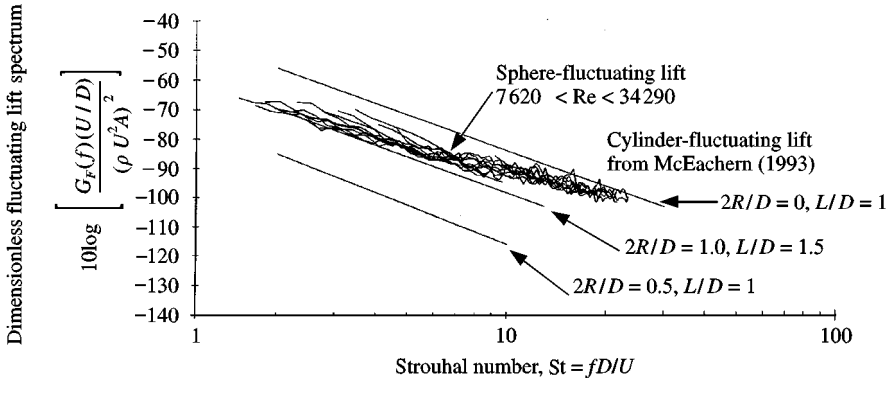

Figure 5. Autospectra of the fluctuating force normalized on the inertial force and time scales of the flow. Data are shown for the sphere (7620 < Re < 34 290), and also for a series of cylinders tested previously by McEachern (1993) (4000 < Re < 18 000).

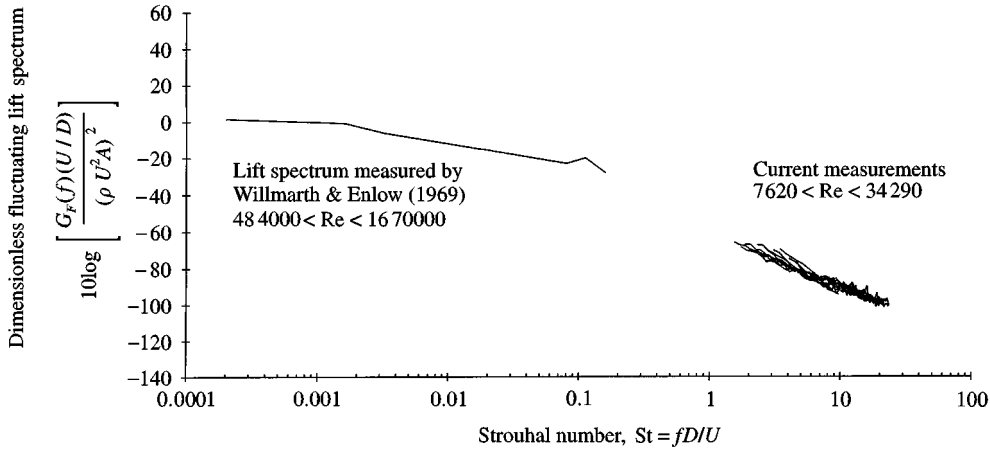

Figure 6. Autospectra of the fluctuating force measured on spheres normalized on the inertial force and time scales of the flow. Data are shown for the current investigation at $1{\cdot}5 < \mathrm{St} < 30$ along with those from the independent investigation of Willmarth & Enlow (1969) at $0{\cdot}0002 < \mathrm{St} < 2$.

investigation at high Strouhal numbers are compared to similarly normalized sphere lift spectra measured by Willmarth & Enlow (1969) at low Strouhal numbers. They performed these measurements on a spherical model operating in a wind tunnel at supercritical Reynolds numbers ($4{\cdot}84 \times 10^5 \leq \mathrm{Re} \leq 1{\cdot}67 \times 10^6$). Their measured Strouhal number range was from approximately 2×10^{-4} to $0{\cdot}2$. Note that a narrow band of energy exists for $\mathrm{St} \sim 0{\cdot}15$ which is due to the lower vortex shedding mode discussed in Section 2.

5. CONCLUSIONS

An experimental investigation of the flow-induced fluctuating side-to-side lift force generated by a sphere set in uniform rectilinear motion has been described. A 7·62 cm diameter spherical sensor was tested in a specially designed low-noise tow tank that was filled with clean, fresh water. Empirical scaling laws, based on the classical unsteady lift coefficient, were used that allow the measured flow-induced fluctuating force frequency spectra to be collapsed to a reasonable single curve. In particular, for the Reynolds number range of $7620 < \mathrm{Re} < 34\,290$, the unsteady forces were found to scale on the inertial forces created by turbulent flow near the sphere. The frequencies scale on the inertial time scale D/U under these conditions and, for $\mathrm{St} > 1{\cdot}5$, the spectra are broadband. Based on flow visualization, Taneda (1978) speculated that a sphere should generate a significant random lift force due to a non-axisymmetric wake that rotates randomly (Achenbach 1974) around the axis of mean flow. The results presented here support that claim, in that a broadband random lift coefficient is clearly measurable.

The nondimensional lift spectra measured for the sphere are similar to those measured in earlier investigations on a finite-length cylinder with various endcap geometries. The main difference between the two data sets is that the spectral levels roll off slightly faster for the cylinders as St increases. The right-circular cylinder in cross flow creates approximately 10 dB more spectral energy than does the sphere for $2 < \mathrm{St} < 10$. An optimum cylinder endcap radius exists, and the side force spectral levels measured on a cylinder with this geometry are at least 20 dB lower than those of the sphere.

ACKNOWLEDGEMENTS

The work reported here has been supported by the Naval Air Warfare Center, Aircraft Division, Patuxent River, MD, and the Office of Naval Research, Code 321-SS. The authors are indebted to Drs James McEachern and Thomas Gabrielson for numerous fruitful discussions pertaining to this research.

References

Achenbach, E. 1974 Vortex shedding from spheres. *Journal of Fluid Mechanics* **62,** 209–221.

Berliner, M. J. & Lindberg, J. F. (eds) 1995 *Acoustic Particle Velocity Sensors*: *Design*, *Performance*, *and Applications*, AIP Conference Proceedings 368, American Institute of Physics, Woodbury, NY, U.S.A. p. vii.

Blake, W. K. 1986 *Mechanics of Flow-Induced Sound and Vibration*, Vol. 1, p. 240, Orlando: Academic Press.

Finger, R. A., Abbagnaro, L. A. & Bauer, B. B. 1979 Measurement of low-velocity flow noise on pressure and pressure gradient hydrophones. *Journal of the Acoustical Society of America* **65,** 1407–1412.

Gabrielson, T. B., McEachern, J. F. & Lauchle, G. C. 1995a Underwater acoustic intensity probe. United States Patent 5,392,258.

Gabrielson, T. B., Gardner, D. L. & Garrett, S. L. 1995b A simple neutrally buoyant sensor for direct measurement of particle velocity and intensity in water. *Journal of the Acoustical Society of America* **97,** 2227–2237.

Jones, A. R. 1996 Flow-induced self noise on spherical and cylindrical sensors. M.S. Thesis, Graduate Program in Acoustics, Pennsylvania State University, University Park, PA, U.S.A.

Keller, B. D. 1977 Gradient hydrophone flow noise. *Journal of the Acoustical Society of America* **62,** 205–208.

Kim, H. J. & Durbin, P. A. 1988 Observations of the Frequencies in a sphere wake and of drag increase by acoustic excitation. *Physics of Fluids* **31,** 3260–3265.

McEachern, J. F. 1980 Experimental development of a compact flow shield. Institute of Electrical and Electronics Engineering Publication 80CH 1578-4 AES, 38–41.

McEachern, J. F. 1993 The effects of body geometry on the flow noise of cylinders in cross flow. Ph. D. Dissertation, Graduate Program in Acoustics, Pennsylvania State University, University Park, PA, U.S.A.

McEachern, J. F. & Lauchle, G. C. 1995 Flow-induced noise on a bluff body. *Journal of the Acoustical Society of America* **97,** 947–953.

Möller, W. 1938 Experimentelle untersuchung zur hydromechanik der kugel. *Physik Zeitschrift* **39,** 57–80.

Sakamoto, H. & Haniu, H. 1990 A study on vortex shedding from spheres in uniform flow. *ASME Journal of Fluids Engineering* **112,** 386–392.

Taneda, S. 1956 Experimental investigation of the wake behind a sphere at low Reynolds numbers. *Journal of the Physical Society of Japan* **11,** 1104–1108.

Taneda, S. 1978 Visual observations of the flow past a sphere at Reynolds numbers between 10^4 and 10^6. *Journal of Fluid Mechanics* **85,** 187–192.

Willmarth, W. W. & Enlow, R. L. 1969 Aerodynamic lift and moment fluctuations of a sphere. *Journal of Fluid Mechanics* **36,** 417–432.